CHEMPHYSCHEM

DOI: 10.1002/cphc.201000788

Validation of DFT-Based Methods for Predicting Qualitative Thermochemistry of Large Polyaromatics

Karen Hemelsoet,*[a] Freija De Vleeschouwer,[b] Veronique Van Speybroeck,[a] Frank De Proft,[b] Paul Geerlings,[b] and Michel Waroquier*[a]

We present a validation of computationally efficient density functional-based methods for the reproduction of relative bond dissociation energies of large polyaromatic hydrocarbons. Through the calculation of intrinsic radical stabilities and the computation of spin densities, the extent of delocalization of the unpaired electron in the benzylic radicals is examined. We focus on the influence of the level of theory choice applied for the geometry optimization and the role of van der Waals corrections on thermochemical properties. The dispersion effects mainly influence the energetics, causing a small upward shift of the bond dissociation energies. The long-range corrected CAM-B3LYP functional does not improve the traditional B3LYP results for the geometry description of the large delocalized radicals, however a non-negligible influence was encountered when applied for the energetics. It is reported that the f polarization functions present in the 6-311 + G(3df,2p) basis set lead to an erroneous trend when combined with the B2PLYP functional for the computation of the single point energies.

1. Introduction

Polycyclic aromatic hydrocarbons (PAHs) are amongst the most widely studied organic molecules, both from an experimental and theoretical point of view.[1–3] They are the largest known class of chemical carcinogens and mutagens.[4–7] Their origin can be natural—they are found as traces in atmospheric aerosols and many celestial objects,[8–11] or anthropogenic—they are formed during the formation of soot or coal conversion processes.[12–16] Our interest stems from their importance as key intermediates in the coke formation process during steam cracking.[17–24] In particular, we have used various polyaromatic structures to model the coke surface and to study carbon–hydrogen bond dissociation properties and corresponding hydrogen abstraction reactions from both pure and methylated PAHs.

A recent thorough theoretical study by Hajgató et al. is of particular interest for the present paper since it provides detailed information on the true physical nature of the important class of polyacenes.[25] It was (re)stated that all investigated *n*-acenes ($n = 1$ to 7) exhibit a ^1A_g singlet closed-shell electronic ground state as opposed to the open-shell singlet biradical nature which has been previously conjectured. The latter conclusion was however an artefact due to the instability of unrestricted wave functions in conjunction with rather modest basis sets. Singlet–triplet gaps, both vertical and adiabatic, could be determined very accurately by Hajgató et al. using an extrapolation to the highly accurate CCSD(T)/cc-pV∞Z level.[25] Other theoretical studies on aromatic molecules (with most emphasis on benzene) have revealed that ab initio methods such as MP2, MP3, CISD, and CCSD, combined with particular basis sets predict anomalous, non-planar equilibrium geometries whereas the planar structures are characterized to exhibit at least one imaginary frequency.[26,27] This irregularity is due to an insidious intramolecular basis set incompleteness error (BSIE). Moran et al. argued that only correlated wave functions are susceptible to this BSIE. This problem is not observed for the series of better balanced Dunning's correlation consistent basis sets.[26]

Due to their challenging characteristics, PAHs are also considered as interesting test molecules to assess the performance of newly developed theoretical models. In a recent article, Neese et al. present an efficient implementation of a modified MP2 technique, namely the orbital-optimized spin-component scaled second-order Møller–Plesset perturbation theory (OO-SCS-MP2).[28] MP2-based methods become computationally feasible for systems of moderate size due to efficient implementation treatments such as the resolution of the identity (RI) approximation.[29] The performance of the aforementioned OO-SCS-MP2 approach was extensively benchmarked using three different test sets, giving special attention to situations where spin contamination in the unrestricted Hartree–Fock part substantially reduces the quality of the computation of the MP2 correlation energy.[28] It was found that the orbital optimization drastically improves the accuracy and stability of the parent

[a] Dr. K. Hemelsoet, Prof. Dr. V. Van Speybroeck, Prof. Dr. M. Waroquier
Center for Molecular Modeling, Ghent University
Technologiepark 903, B-9052 Zwijnaarde (Belgium)
QCMM-alliance, Ghent-Brussels (Belgium)
Fax: (+32) 9-264-65-60
E-mail: Karen.Hemelsoet@UGent.be
Michel.Waroquier@UGent.be

[b] Dr. F. De Vleeschouwer, Prof. Dr. F. De Proft, Prof. Dr. P. Geerlings
Eenheid Algemene Chemie (ALGC)
Faculteit Wetenschappen, Vrije Universiteit Brussel
Pleinlaan 2, B-1050 Brussels (Belgium)
QCMM-alliance, Ghent-Brussels (Belgium)

Supporting information for this article is available on the WWW under http://dx.doi.org/10.1002/cphc.201000788.

nonorbital-optimized methods in electronically difficult situations, inherently at a higher computational cost. One of the three chosen test sets involves two large methylated PAHs for which carbon–hydrogen bond dissociation properties are calculated. These systems have originally been investigated by some of the present authors, where it was indeed noted that HF and post-HF calculations on the resulting open-shell radicals are largely hampered due to spin contamination.[23] The B3P86 and BMK functionals were found to provide good energetics when benchmarked with G3(MP2)-RAD data.

In addition to studies focussing on post-HF variants, the use of DFT-based methods remains often preferred when studying systems of large size. Developments such as the inclusion of dispersion interactions[30–32] have boosted assessment studies in recent years.[33–40] The present contribution is dealing with large polyaromatic systems and derived radicals, and hence the failure of most commonly applied DFT functionals to describe the latter radicals should be taken into account. This failure is due to the delocalization error which leads to an unphysical energy underestimation.[41–43] Johnson et al. have constructed two new functionals rCAM-B3LYP and MCY3 with minimal electron delocalization error.[44] Herein, we test the performance of the CAM (Coulomb-attenuating method)-B3LYP functional, which is a hybrid functional with improved long-range properties.[45] The functional has been shown to provide significantly better Rydberg and charge transfer electronic excitation energies. Moreover, its performance for a wider range of properties and molecules was assessed by Peach et al.,[46] demonstrating the improved description of electronic polarisabilities, which is consistent with the long-range nature of this property. This was furthermore shown for the important class of polyacetylene oligomer chains (size up to $C_{24}H_{26}$) and its donor–acceptor substituted counterparts.[47–49] The performance of this long-range corrected functional for the determination of the mechanochemical strength of covalent bonds was assessed by Iozzi et al. However, a superior behavior of pure DFT methods over B3LYP and CAM-B3LYP was obtained.[50]

Herein we focus on the reliable computation of bond dissociation energies of systems for which a substantial delocalization of the radical center is observed. Some of the present authors recently generalized the concept of an intrinsic radical stability scale, based on computed bond dissociation enthalpies that are broken down into parts that only incorporate properties of the individual radical fragments, such as intrinsic radical stabilities, a radical electrophilicity term and a local Pauling electronegativity term.[51,52] This model explains 96% of the magnitude of the BDEs and a mean absolute deviation of 15.3 kJ mol^{-1} is observed[52] when a comparison was made with available experimental results, whereas the BDEs directly computed from first principles show a deviation of 9.8 kJ mol^{-1} for the same set of experimental data. Other studies often use relative BDEs to determine radical stability sequences.[35,53–57] In the case of the investigated PAHs, intrinsic radical stabilities can be related to the degree of delocalization within these large-sized radical systems.

The article is organized as follows. First, the extent of delocalization and related intrinsic stability is elucidated using B3LYP optimized geometries. Second, the influence of the level of theory used for the geometry optimization is examined. Third, various energy refinement methods are assessed, with special emphasis on the use of explicit dispersion corrections and the long-range corrected CAM-B3LYP and LC-ωPBE functionals, complementing the information obtained from the analysis of the intrinsic radical stabilities.

Computational Details

Calculations have been performed using the Gaussian 03[58] and Orca[59] packages. All computations involving the open-shell radical species were performed using the unrestricted methodology, unless noted otherwise. Herein bond dissociation energies, without vibrational and thermal corrections to the electronic energies are reported to allow a straightforward comparison with the results from ref. [28]. These corrections can amount to 30 kJ mol^{-1} and are reported in the Supporting Information. All structures are initially optimized at the B3LYP/6-31+G(d,p) level of theory. The B3LYP functional has previously been shown to provide good geometries for hydrocarbons, for example, refs. [34, 35, 60, 61].

Intrinsic radical stabilities were estimated using Equation (1):[52]

$$\mathrm{BDE(A-B)} = \begin{cases} (\mathrm{stab_A} + \mathrm{stab_B} + a\Delta\omega_\mathrm{A}\Delta\omega_\mathrm{B}), & \text{if } \chi_\mathrm{A} < 0 \text{ and } \chi_\mathrm{B} < 0 \\ (\mathrm{stab_A} + \mathrm{stab_B} + a\Delta\omega_\mathrm{A}\Delta\omega_\mathrm{B} + b\Delta\chi_\mathrm{A}\Delta\chi_\mathrm{B}), & \text{otherwise} \end{cases}$$

According to this model, the bond dissociation enthalpy (BDE) of the homolytic splitting of the molecule A–B into the fragments A and B can be split into three parts, namely the sum of the stabilities of A and B, a global term combining the electrophilicities ($\Delta\omega$) of A and B and a local term involving the Pauling electronegativities ($\Delta\chi$) of the radical centers of A and B. More information can be found in ref. [52], using B3LYP/6-311+G(d,p) geometries and B3P86/6-311+G(d,p) energetics for the bond dissociation enthalpies and B3LYP/6-311+G(d,p) energies for the electrophilicities. Herein, the same level of theory was applied for the energetics, while the B3LYP/6-31+G(d,p) method was used for the geometries (only small deviations were found comparing both basis sets). In the remainder of this manuscript, use is made of the standard notation LOT-E//LOT-G with LOT-E and LOT-G being the electronic levels of theory (LOT) used for the energetics and geometry optimizations, respectively.

The influence of the geometry optimization on resulting bond dissociation energies is assessed using B3P86/6-311G(d,p) energetics. The good performance of this level of theory for the accurate reproduction of carbon–hydrogen bond dissociation properties was previously established.[19,23] In particular, C–H bond dissociation enthalpies of a series of large polyaromatics (including the molecules studied in the present work) were computed using the B3P86, BMK and M05-2X functionals.[23] The assessment was based on two grounds. First a comparison was made in the case of the C-H BDE of toluene, for which experimental values are available and for which we computed a high-level W1 value. Second, a comparison was made with computed G3(MP2)-RAD data for toluene, singly methylated naphthalene and anthracene and it was found that the three functionals were able to provide correct chemical trends. Overall, the B3P86 functional shows the best performance, followed by BMK and M05-2X. Herein, the B3LYP/6-31+G(d,p) geometries are compared with those using a 6-311G(d,p) and tzvp basis set. The influence of an empirical dispersion correction

(B3LYP-D) is also addressed (*xyz* coordinates of these optimized structures can be found in the Supporting Information).[30] Additional CAM-B3LYP[45] optimizations were performed using the Gaussian 09 package.[62] The CAM-B3LYP functional comprises 0.19 Hartree–Fock (HF) plus 0.81 Becke 1988 (B88) exchange interaction at short range and 0.65 HF plus 0.35 B88 at long range.[45] The intermediate region is smoothly described through the standard error function with parameter $0.33\,a_0^{-1}$.

Using B3LYP-D/tzvp optimized geometries, subsequent energy calculations were performed with two DFT functionals, in particular the B3LYP and BP86 methods. These were selected based on their availability within the Orca software package and used in combination with the tzvpp basis set which introduces 2d and 1f polarization sets on each heavy atom together with 2p and 1d sets on each hydrogen. The B3LYP/G implementation in Orca is applied. B2PLYP-D calculations were also performed, using the RI approximation for the Coulomb part as well as for the second-order perturbation part. In these cases, the tzvpp basis was extended with matching auxiliary basis sets.

CAM-B3LYP energy calculations were also performed and compared with standard B3LYP values in order to assess the influence of long range effects on carbon-hydrogen bond dissociation energies. A slow convergence pattern was obtained in the case of calculations using the large 6-311+G(3df,2p) basis set and hence also the 6-311+G(d,p) variant was applied. Finally, additional LC-ωPBE calculations were performed.[63–66]

In the online Supporting Information the C–H bond dissociation energies (in $kJ\,mol^{-1}$), taken from ref. [28] or derived from ref. [23] for the investigated molecules, thermal corrections to the enthalpy [in $kJ\,mol^{-1}$] on the resulting bond dissociation energies [B3LYP/6-31+G(d)] and *xyz* coordinates of the optimized B3LYP-D/tzvp geometries of the reactants and radicals are available.

2. Results and Discussion

Singly methylated PAHs are examined in detail. The molecules are schematically shown in Figure 1 and represent examples of a large linear (**5**) and non-linear (**10**) methylated aromatic. The methylation can occur at different positions (indicated by numbers as given in Figure 1). Overall, seven singly methylated PAHs are investigated herein.

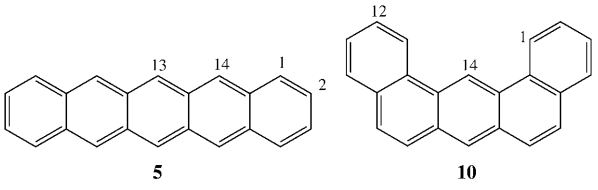

Figure 1. Singly methylated PAHs. Methylated positions, where bond dissociations in the methyl groups are considered, are indicated by numbers. The same labeling as in refs. [23] and [28] has been used.

2.1. Geometry Optimization

The optimized B3LYP/6-31+G(d,p) geometries of all methylated reactant structures of molecule **5** were found to be planar, as well as molecule **10**–**12**. Reactant **10**–**1** exhibits modest deviations from planarity, whereas steric hindrance between the methyl group and the aromatic structure leads to a clearly non-planar, curled up structure in case of **10**–**14**. For the corresponding radicals resulting from the C-H dissociation in the methyl groups, substantial deviations from planarity are obtained in case of **5**–**13**, **5**–**14**, **10**–**1** and **10**–**14**.

In order to check the validity of a single-reference treatment of the investigated large polyaromatics, the multiplicity of all reactants and radicals was changed and the corresponding structures were again optimized to obtain adiabatic (*AD*) energy gaps. Vertical (*VE*) energy gaps were also obtained using single-point energy calculations on the initial optimized geometries. It is seen from Table 1 that in all cases the singlet and doublet structures (for the reactants and radicals, respectively) are energetically favored over the triplet and quadruplet states. The large energy differences for both the vertical and adiabatic energy gaps point out that a single-determinant description as applied in DFT is suited for the systems under investigation. The computed data of **5** are in line with the results reported in ref. [25] for the (non-methylated) linear pentacene molecule, exhibiting a vertical and adiabatic excitation energy of 131.8 and 101.2 $kJ\,mol^{-1}$, respectively. The latter values have been obtained at the very accurate CCSD(T)/cc-pV∞Z level of theory.

Table 1. Energy differences [$kJ\,mol^{-1}$] between the singlet and triplet state (for the reactants) and the doublet and quadruplet state (for the radicals), computed at the B3LYP/6-31+G(d,p) level of theory.

	ΔE(S–T)		ΔE(D–Q)	
	VE	*AD*	*VE*	*AD*
5–**13**	−92.1	−71.8	−243.5	−190.7
5–**14**	−95.3	−74.7	−184.5	−146.2
5–**1**	−97.0	−76.3	−120.4	−98.8
5–**2**	−97.3	−76.5	−128.5	−105.8
10–**14**	−241.1	−197.5	−308.4	−255.8
10–**1**	−255.1	−226.5	−246.4	−215.3
10–**12**	−643.2	−612.5	−257.9	−227.0

2.2. Delocalization of the Radical Center

A useful measurement of the degree of delocalization within PAHs is to compute the intrinsic stability of the large radical systems via a rather simple model as introduced by some of the authors of this article.[52] The model uses bond dissociation enthalpies of the molecule A–B, as well as electrophilicities[51,67] and Pauling electronegativities of A and B to estimate the stability of a certain radical A, irrespective of its radical partner B. This implies that the intrinsic stability of the new radical can be obtained on the basis of the computation of only the global electrophilicity of this new radical and 1 BDE, for instance PAH–H. It might, however, be advisable to estimate the radical stability using three BDEs, for example, by combining the radical with a (strongly) nucleophilic (e.g. hydroxymethyl), a neutral (e.g. hydrogen), and a (strongly) electrophilic (e.g. fluorine) radical to guarantee that the influence of different chemical environments is properly taken into account. This

model has proven its value not only for radical systems,[52,68] but also for other highly reactive species that display some sort of radical character (such as the divalent silylenes and biradical *p*-benzynes).[69]

Table 2 contains the intrinsic stabilities for the different PAHs in this work (Figure 1), resulting from radical combinations with the strongly nucleophilic CH_2OH, the neutral H and the electrophilic F radical. The larger is the value for the stability

Table 2. Intrinsic radical stabilities (stab) [kJ mol^{-1}] using B3P86/6-311+G(d,p)//B3LYP/6-31+G(d,p) bond dissociation enthalpies and B3LYP/6-311+G(d,p)//B3LYP/6-31+G(d,p) electrophilicities.

5–13	67.4	**10–14**	91.3
5–14	78.7	**10–1**	127.5
5–1	112.0	**10–12**	129.4
5–2	111.3		

property (stab), the less stable is the radical. From these data is it seen that the site of methylation has a big influence on the stability of the obtained radicals. Comparison with the previously established radical stability scale (see Figure 2) shows that the PAH radicals, and especially **5–13**, **5–14** and **10–14**,

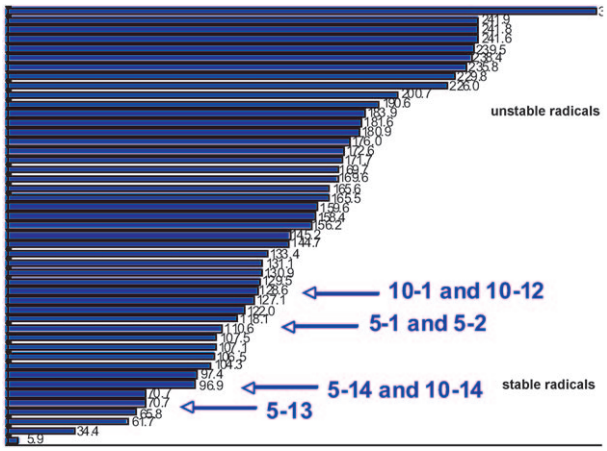

Figure 2. Comparison of the PAH radical stabilities with the radical stability scale of reference [52].

should be classified as very stable. If we take the benzyl radical with an intrinsic stability of 130.9 kJ mol^{-1}, as the reference system, all PAH radicals are identified as (much) more stable species, except for the radicals **10–1** and **10–12**. For the latter two systems, we expect delocalization only over the first ring.

In order to get a more visual picture of the degree of delocalization of the unpaired electron, spin densities and spin atomic charges of the investigated benzylic radicals were calculated using the natural population analysis (NPA) scheme.[70] The results are depicted in Figure 3. The benzyl radical, as a reference

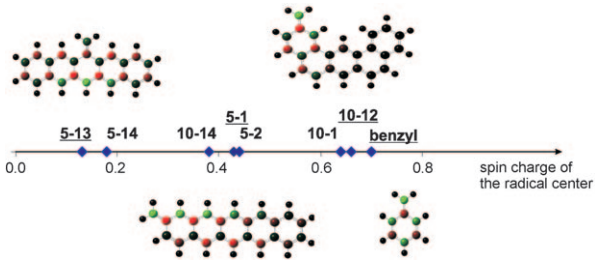

Figure 3. Atomic spin charge of the radical center for the various large radicals and the reference benzyl radical, calculated at the B3LYP/6-311+G(d,p)//B3LYP/6-31+G(d,p) level of theory. Spin densities are also visualized for the underlined radicals. A continuous coloring range is applied: green and red refer to positive and negative values of the spin density, respectively; whereas black atoms are spin neutral.

system, is also shown. Compared to the reference system, the spin charge on the radical center has decreased substantially:

$$5-13 < 5-14 \ll 10-14 < 5-1 < 5-2 \ll 10-1 < 10-12 < \text{benzyl}$$

This order is completely in line with the results from the computed intrinsic stabilities (Figure 4). The spin charge on the radical center correlates well with the intrinsic stabilities of the radicals with a correlation coefficient of 95%.

From Figure 3 it can be seen that the observed delocalization behavior is highly dependent on the position of methylation and on the degree of planarity of the aromatic structure (which will be discussed in more detail in Section 2.3.1). The planar radicals **5–1** and **5–2** exhibit delocalization over the ring where the extra CH_2 group is attached, as well as over the second, third (and to less extent fourth) ring. In the fifth ring the spin density can be considered as negligible. For the nonplanar radical **5–13** symmetric behavior is observed with the largest spin density on the opposite carbon atom of the attached CH_2 group. An analogous behavior is seen for **5–14**, with delocalization of the unpaired electron over all five rings.

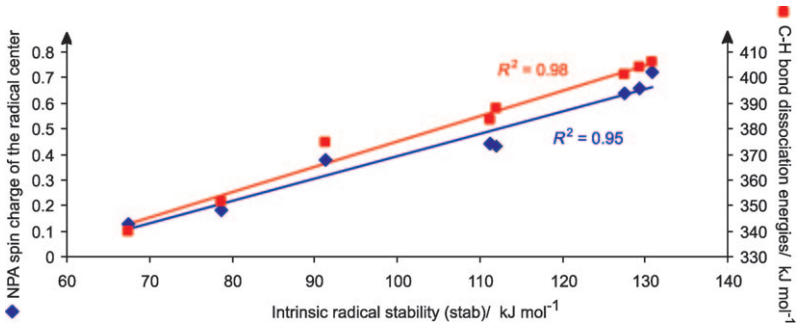

Figure 4. Correlation between the spin charge on the radical center (in blue) and B3P86 bond dissociation energies (in red) versus the intrinsic stabilities for the investigated benzylic radicals, including the reference benzyl radical.

In case of radicals **10**–**1** and **10**–**12**, hardly any delocalization is observed outside the ring containing the CH_2 group. The behavior hence resembles most the reference benzyl radical, explaining the close values concerning the intrinsic stabilities. The delocalization over the extra rings is more pronounced in case of radical **10**–**14**. We expect the differences in delocalization pattern of the unpaired electron to be reflected in the degree of underestimation of the DFT energies of the radicals. However, based on the analysis of the radicals, we can not predict the behavior of the bond dissociation energies as the latter depend on the relative dissociation error of both the reactant PAH and product radical.

Table 3. C–H bond dissociation energies [kJ mol^{-1}] using B3P86/6-311G(d,p) energies as a function of level of theory used for the geometry optimization.

	B3LYP			CAM-B3LYP	B3LYP-D
	6-31+G(d,p)	6-311G(d,p)	tzvp	6-31+G(d,p)	tzvp
Toluene	405.9				
5–**13**	339.7	340.8	340.4	340.4	339.8
5–**14**	351.8	351.6	352.7	351.8	352.7
5–**1**	387.8	387.4	386.3	385.9	387.5
5–**2**	383.4	382.7	382.7	382.4	382.9
10–**14**	374.6	374.6	373.8	375.4	373.6
10–**1**	401.1	401.2	403.3	401.0	403.1
10–**12**	404.0	401.5	401.7	402.0	401.8

2.3. Bond Dissociation Energies

2.3.1. Influence of the Geometry Optimization

Previous studies focusing on hydrogen abstraction reactions on hydrocarbons already extensively tested the influence of the level of theory for the geometry optimization. It was found that its influence is rather small, except for HF and MP2 methods where one is confronted with additional problems.[34,61] Moreover, hybrid DFT methods provide excellent low-cost performance for larger molecules as are structures **5** and **10** (Figure 1). To reassess these statements for the present molecules, C–H bond dissociation energies were calculated on a set of geometries optimized using different levels of theory.

The influence of the basis set is addressed testing three different basis sets, in particular 6-31+G(d,p), 6-311G(d,p) and tzvp. We want to note that in the case of the 6-31+G(d,p) basis set, the inclusion of diffuse functions (of sp character) also leads to a tzvp-type basis set and hence large differences between these basis sets are not expected. The optimized geometries (all in combination with the B3LYP functional) show minor differences. Figure 5 displays the geometries of radicals **5**–**13** and **10**–**14**, serving as illustrative examples for the non-planar structures which are expected to be more prone to variations in the basis set and inclusion of dispersion effects. The variation of the relevant dihedral angle C2–C3–C4–C5 is negligible, ranging between 23.2 and 24.2° for **5**–**13** and 36.3 and 36.5° for **10**–**14**. Consequently, the geometry optimization using a basis set of double- or triple-ζ quality has a minor effect on the bond dissociation energies as can be seen in Table 3. The highest difference is found for molecule **10**–**12**, the B3LYP/6-31+G(d,p) on one hand and the B3LYP/6-311G(d,p) geometry on the other hand result in bond dissociation energies differing by 2.5 kJ mol^{-1}.

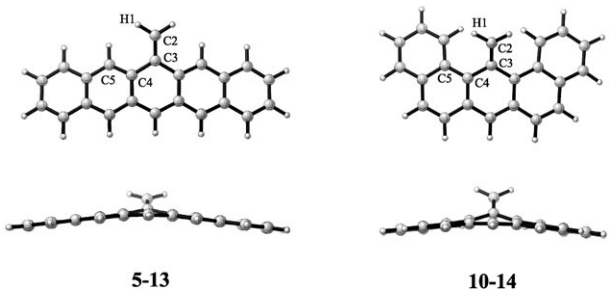

Figure 5. Top and side view of radicals **5**–**13** and **10**–**14** with labeling of dihedral angles.

As we are dealing with large delocalized radicals, CAM-B3LYP/6-31+G(d,p) optimizations were also performed to check whether the long-range correction has a substantial influence on the geometries. This is manifestly not the case: values of dih(C2–C3–C4–C5) amount to 24.0 and 36.3° for **5**–**13** and **10**–**14**, respectively. The effect on the resulting carbon–hydrogen bond dissociation energies is hence also negligible (Table 3). Similarly, from Table 3 it is seen that the inclusion of explicit dispersion corrections using the B3LYP-D methodology also alters the bond dissociation energies only slightly, even for an internally sterically hindered molecule such as **10**.

2.3.2. Influence of Energy Refinements and Single-Point Dispersion Effects

We now examine the performance of various levels of theory for the qualitative and/or quantitative reproduction of bond dissociation energies. Unfortunately, no experimental data are available for carbon-hydrogen dissociation of these large methylated aromatics. Hence, the recently reported OO-SCS-MP2 results are taken as a benchmark.[28] An overview of available literature values of bond dissociation energies of molecules **5** and **10** is given in the Supporting Information. Figure 6 displays the relative behavior of the dissociation properties as a function of the methylated position. It should be stressed that the data are based on different geometries and different levels of theory for the energetics as outlined in Figure 6. Generally speaking, the observed trend of bond dissociation energies shows an increase of 15 kJ mol^{-1} from **5**–**13** to **5**–**14**,[71] then a larger increase of 40 kJ mol^{-1} to **5**–**1**, and the step from **5**–**1** to **5**–**2** leads to a decrease of about 5 kJ mol^{-1}. The bond is strengthened by about 25 kJ mol^{-1} going from **10**–**14** to **10**–**1**, and there is little difference between **10**–**1** and **10**–**12**.

Basis Set Effects

Figure 6 also reports post-HF results taken from refs. [28] and [23] and it is seen that the various levels of theory show the same qualitative behavior, but for one manifest exception,

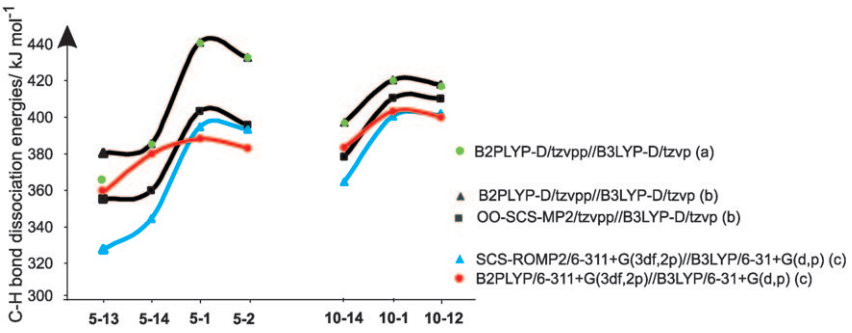

Figure 6. C–H bond dissociation energies of molecules **5** and **10**: a) this work,[71] b) ref. [28], c) ref. [23].

namely the B2PLYP predictions using the 6-311+G(3df,2p) basis set (red curve in Figure 6). We previously disregarded these data since the radicals are heavily spin-contaminated. Nevertheless, the large $<S^2>$ values do not explain why the relative trend is not correctly reproduced. This was also pointed out by Neese et al., whose B2PLYP-D/tzvpp data show no peculiarities. We therefore closely inspected the original computations and it was observed that the B2PLYP/6-311+G(3df,2p) discrepancies can be traced back to an erroneous underestimation of the energy for the large π-radicals corresponding to **5**–**1**, **5**–**2**, **10**–**1** and **10**–**12**. The resulting bond dissociation energy values are thus underestimated to the same extent. Various basis sets were tested, including some that lead to the aforementioned BSIE for benzene in ref. [26]. However, taking into account that we only vary the basis set for the energy calculations, it was concluded that only the 6-311+G(3df,2p) variant predicts a significantly different behavior. More specifically, omitting the f polarization functions on the hydrogen atom in the large basis set leads to a correct picture as shown in Figure 7 for molecule **5** where C–H bond dissociation energy differences are depicted relative to the value of molecule **5**–**13**. The irregular behavior of the large 6-311+G(3df,2p) basis set is an illustration of the main drawback of the series of Pople-type basis sets, that is, they do not converge towards a basis set limit with increasing size. This is partly because no higher-*l* functions are included, and because the construction of larger basis sets (through inclusion of quite different Gaussian-type orbitals) is based on physical properties rather than in a consistent fashion. This is in contrast to the Dunning-type basis sets. However, the latter equivalents of triple-zeta quality augmented with diffuse and polarization functions are computationally unfeasible for systems of this size. The reported basis set effect is not observed for the DFT-based calculations.

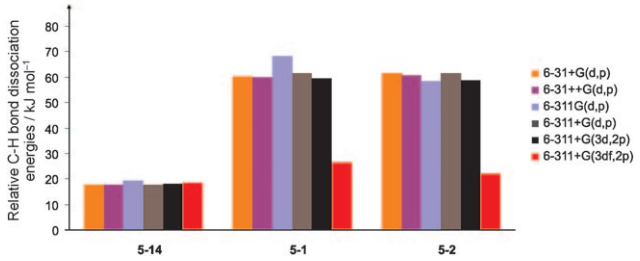

Figure 7. C–H bond dissociation energies [kJ mol^{-1}] of molecule **5**, relative to the value of **5**–**13**. B3LYP/6-31G(d,p)-optimized geometries and B2PLYP energies in combination with various basis sets.

Explicit Inclusion of Dispersion Contributions

It was reported in ref. [28] that low-cost DFT methods show the correct qualitative trend, however the quantitative agreement with the post-HF methods such as OO-SCS-MP2 varies considerably. New calculations have been done based on B3LYP-D/tzvp-optimized geometries to address the inclusion of van der Waals contributions. The BP86 and B3LYP functionals are combined with a tzvpp basis set, the results with and without dispersion corrections are reported. The applied methodology is identical to ref. [28] to allow a transparent comparison with the OO-SCS-MP2 results.[28] The data are given in Table 4

Table 4. C–H bond dissociation energies [kJ mol^{-1}].

	Method/tzvpp//B3LYP-D/tzvp				
	OO-SCS-MP2[28]	BP86	B3LYP	BP86-D	B3LYP-D
5–13	357.3	334.1	325.0	339.1	330.0
5–14	361.5	344.3	337.0	349.2	341.9
5–1	400.4	375.9	372.8	379.7	376.6
5–2	393.7	370.9	368.1	373.6	370.8
10–14	378.2	361.7	359.4	368.8	366.5
10–1	407.1	388.1	387.1	393.3	392.2
10–12	406.7	390.4	386.9	392.9	389.4

and displayed in Figure 8. It is illustrated that the qualitative trend is again correctly reproduced by all levels of theory. Larger deviations are obtained for the linear methylated molecule **5** compared to the non-linear structure **10**. Inclusion of van der Waals corrections leads to slightly larger bond dissociation energies. The average increase equals 4.4 kJ mol^{-1} for the tested functionals. This small shift is nevertheless not sufficient to obtain accurate quantitative data. The underestimation of the bond dissociation energies in case of DFT functionals can hence only be partially overcome through inclusion of explicit van der Waals effects. Overall, it is concluded that the B3P86 results (derived from ref. [23] and tabulated in Table 3 and Figure 8) are closest to the OO-SCS-MP2 values.

Long-Range Corrected Functionals

The observed energy underestimation of strongly delocalized radicals is one of the shortcomings of most DFT functionals

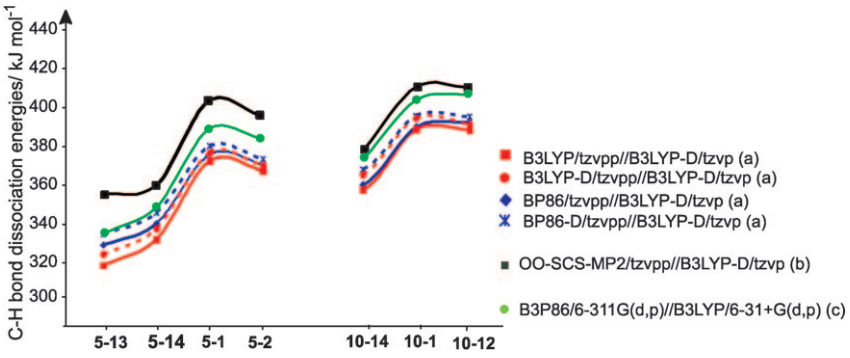

Figure 8. C–H bond dissociation energies of molecules **5** and **10**: a) this work, b) ref. [28], c) ref. [23].

and is of great importance for the investigated class of molecules. We thus tested the performance of the long-range corrected CAM-B3LYP functional by comparison with B3LYP energetics. The obtained data [using the B3LYP/6-31+G(d,p) optimized geometries] are tabulated in Table 5. In case of the linear methylated molecule **5**, CAM-B3LYP/6-311+G(3df,2p) predicts an average decrease of 4.2 kJ mol^{-1}, which is in the wrong direction with respect to the reference OO-SCS-MP2 values. However, in case of molecule **10**, we get the opposite and a required increase (average of 6.7 kJ mol^{-1}) is observed comparing CAM-B3LYP with B3LYP. Convergence problems were noticed for this large Pople-type basis set, and hence we also performed calculations using the 6-311+G(d,p) basis set. Similar conclusions were obtained, that is, the mean average difference between the CAM-B3LYP and B3LYP data equals −3.4 and 6.6 kJ mol^{-1} for structures **5** and **10**, respectively. Moreover, additional LC-ωPBE calculations (exhibiting 100% exact exchange at long distance) also do not succeed in reproducing the OO-SCS-MP2 data more accurately. Despite the clear differences in extent of delocalization of the unpaired electron (e.g. for molecule **10** the extended delocalization in case of **10**–**14** versus the limited delocalization in case of **10**–**1** and **10**–**12**), this is not reflected in the performance of both long-range corrected functionals. The final correction due to the long-range corrected density functionals is most probably the result of the subtle balance of delocalization effects in the PAH and the resulting radical. In addition, it should be remarked that the difference between the B3LYP and CAM-B3LYP bond dissociation energies amounts to 8 kJ mol^{-1} at most for the present set of compounds.

Table 5. C–H bond dissociation energies [kJ mol^{-1}] using B3LYP/6-31+G(d,p)-optimized geometries.

	6-311+G(d,p)			6-311+G(3df,2p)	
	B3LYP	CAM-B3LYP	LC-ωPBE	B3LYP	CAM-B3LYP
5–13	325.7	319.4	297.5	324.5	318.8
5–14	337.6	330.0	310.1	336.6	332.4
5–1	373.9	373.3	347.8	374.9	372.6
5–2	369.6	369.3	343.8	372.6	368.1
10–14	360.1	365.8	356.2	360.3	365.3
10–1	387.5	394.1	386.4	386.9	393.6
10–12	388.5	397.5	392.0	390.4	398.7

3. Conclusions

Herein we validate the use of density-functional-based methods for the reliable computation of relative carbon-hydrogen bond dissociation energies of large polyaromatics. The lack of quantitative accuracy of all investigated DFT methods is outweighed by the qualitative agreement. The investigated molecules are shown to be challenging and ideally suited to serve as test systems for systematic improvements of new DFT- or MP2-based methods.

Spin charges and intrinsic radical stabilities indicate the substantial delocalization of the unpaired electron. It is furthermore confirmed that geometries can be optimized using a basis set of double-zeta quality without losing accuracy. Empirical dispersion corrections as well as the use of a long range corrected functional also has a negligible influence on the geometrical parameters. Large excitation energy differences, both vertical and adiabatic, are obtained favoring the singlet and doublet electronic states of the reactant and radical hydrocarbons, respectively.

The inclusion of empirical dispersion effects for the energy computations has a small, but positive effect on the quantitative data when compared with available OO-SCS-MP2 results. The B3P86 functional is the best performing low-cost DFT functional. The long-range corrected CAM-B3LYP functional shows an improvement over regular B3LYP for the investigated non-linear large delocalized radicals, whereas this is not the case for the linear variants. The LC-ωPBE functional also does not succeed in a systematic improvement. The deviating behavior of the B2PLYP/6-311+G(3df,2p) energetics is attributed to the f polarization functions present in this large Pople type basis set, and this specific combination should hence be avoided. Finally, intrinsic stabilities are in line with the bond dissociation properties and indicate the largest stability for the linear radicals with CH_2 groups sited at the inner rings.

Acknowledgements

We wish to acknowledge the Fund for Scientific Research—Flanders (FWO), the Research Board of Ghent University and the Free University of Brussels (VUB) for continuous support. This work is also supported by the IAP-BELSPO project in the frame of IAP 6/27. Computational resources and services used in this work were provided by Ghent University. F.D.V. wishes to acknowledge the Research Foundation—Flanders (FWO) for a post-doctoral fellowship. We also wish to acknowledge stimulating and helpful discussions with Prof. D. J. Tozer.

Keywords: ab initio calculations · bond energy · density functional calculations · intrinsic radical stability · polycycles

[1] E. Clar, *Polycyclic Hydrocarbons*, Academic Press, Londen, **1964**; R. G. Harvey, *Polycyclic Aromatic Hydrocarbons*,Wiley-VCH, Weinheim, **1997**.
[2] J. M. Gonzales, C. J. Barden, S. T. Brown, P. v. R. Schleyer, H. F. Schaefer III, Q.-S. Li, *J. Am. Chem. Soc.* **2003**, *125*, 1064 and references therein.
[3] M. D. Watson, A. Fechtenkötter, K. Müllen, *Chem. Rev.* **2001**, *101*, 1267.
[4] R. G. Harvey, *Polycyclic Aromatic Hydrocarbons: Chemistry and Carcinogenicity,* Cambridge University Press, Cambridge, **1991**.
[5] J. L. Durant, W. F. Busby, A. L. Lafleur, B. W. Penman, C. L. Crespi, *Mutat. Res.* **1996**, *371*, 123.
[6] M. F. Denissenko, A. Pao, M. S. Tang, G. P. Pfeifer, *Science* **1996**, *274*, 430.
[7] L. Weisman, T. J. Lee, F. Salama, M. Head-Gordon, *Astrophys. J.* **2003**, *587*, 256.
[8] L. J. Allamandola, *Top. Curr. Chem.* **1990**, *153*, 1.
[9] a) *Polycyclic Aromatic Hydrocarbons and Astrophysics, NATO ASI Ser., Ser. C 191* (Eds.: A. Léger, L. d'Hendecourt, N. Boccara) Reidel, Dordrecht, **1987**; b) J. L. Puget, A. Léger, *Annu. Rev. Astron. Astrophys.* **1989**, *27*, 161.
[10] J. O. Allen, M. Dookeran, K. A. Smith, A. F. Sarofim, K. Taghizadeh, A. L. Lafleur, *Environ. Sci. Technol.* **1996**, *30*, 1023.
[11] F. J. Lovas, R. J. McMahon, J. U. Grabow, M. Schnell, J. Mack, L. T. Scott, R. L. Kuczkowski, *J. Am. Chem. Soc.* **2005**, *127*, 4345.
[12] C. J. Pope, J. A. Marr, J. B. Howard, *J. Phys. Chem.* **1993**, *97*, 11001.
[13] a) H. Richter, O. A. Mazyar, R. Sumathi, W. H. Green, J. B. Howard, J. W. Bozzelli, *J. Phys. Chem. A* **2001**, *105*, 1561; b) H. Richter, W. J. Grieco, J. B. Howard, *Combust. Flame* **1999**, *119*, 1.
[14] S. J. Harris, A. M. Weiner, R. J. Blint, *Combust. Flame* **1988**, *72*, 91.
[15] a) M. Frenklach, D. W. Clary, W. C. Gardiner, S. E. Stein, *Proc. Combust. Inst.* **1985**, *20*, 887; b) M. Frenklach, J. Warnatz, *Combust. Sci. Technol.* **1987**, *51*, 265; c) M. Frenklach, H. Wang, 23rd Int. Symp. Combustion, The Combustion Institute, Pittsburgh, PA, **1990**, 1559; d) M. Frenklach, 26th Int. Symp. Combustion, The Combustion Institute, Pittsburgh, PA, **1996**, 2258.
[16] J. P. Senosiain, *Faraday Discuss.* **2001**, *119*, 173.
[17] S. Wauters, G. B. Marin, *Ind. Eng. Chem. Res.* **2002**, *41*, 2379.
[18] V. Van Speybroeck, M. F. Reyniers, G. B. Marin, M. Waroquier, *ChemPhysChem* **2002**, *3*, 863.
[19] V. Van Speybroeck, G. B. Marin, M. Waroquier, *ChemPhysChem* **2006**, *7*, 2205.
[20] K. Hemelsoet, V. Van Speybroeck, D. Moran, G. B. Marin, L. Radom, M. Waroquier, *J. Phys. Chem. A* **2006**, *110*, 13624.
[21] V. Van Speybroeck, K. Hemelsoet, B. Minner, G. B. Marin, M. Waroquier, *Mol. Simul.* **2007**, *33*, 879.
[22] K. Hemelsoet, V. Van Speybroeck, M. Waroquier, *Chem. Phys. Lett.* **2007**, *444*, 17.
[23] K. Hemelsoet, V. Van Speybroeck, M. Waroquier, *J. Phys. Chem. A* **2008**, *112*, 13566.
[24] K. Hemelsoet, V. Van Speybroeck, M. Waroquier, *ChemPhysChem* **2008**, *9*, 2349.
[25] B. Hajgató, D. Szieberth, P. Geerlings, F. De Proft, M. S. Deleuze, *J. Chem. Phys.* **2009**, *131*, 224321.
[26] D. Moran, A. C. Simmonett, F. E. Leach III, W. D. Allen, P. v. R. Schleyer, H. F. Schaefer III, *J. Am. Chem. Soc.* **2006**, *128*, 9342.
[27] J. M. L. Martin, P. R. Taylor, T. J. Lee, *Chem. Phys. Lett.* **1997**, *275*, 414.
[28] F. Neese, T. Schwabe, S. Kossmann, B. Schirmer, S. Grimme, *J. Chem. Theory Comput.* **2009**, *5*, 3060.
[29] M. Feyereisen, G. Fitzgerald, A. Komornicki, *Chem. Phys. Lett.* **1993**, *208*, 359.
[30] S. Grimme, *J. Comput. Chem.* **2004**, *25*, 1463.
[31] T. Schwabe, S. Grimme, *Phys. Chem. Chem. Phys.* **2007**, *9*, 3397.
[32] Y. Zhao, D. G. Truhlar, *Theor. Chem. Acc.* **2008**, *120*, 215.
[33] E. I. Izgorodina, D. R. B. Brittain, J. L. Hodgson, E. H. Krenske, C. Y. Lin, M. Namazian, M. L. Coote, *J. Phys. Chem. A* **2007**, *111*, 10754.
[34] K. Hemelsoet, D. Moran, V. Van Speybroeck, M. Waroquier, L. Radom, *J. Phys. Chem. A* **2006**, *110*, 8942.
[35] A. S. Menon, G. P. F. Wood, D. Moran, L. Radom, *J. Phys. Chem. A* **2007**, *111*, 13638.
[36] M. D. Wodrich, C. Corminboeuf, P. R. Schreiner, A. A. Fokin, P. v. R. Schleyer, *Org. Lett.* **2007**, *9*, 1851.
[37] Y. Zhao, D. G. Truhlar, *J. Chem. Theory Comput.* **2008**, *4*, 1849.
[38] M. Korth, S. Grimme, *J. Chem. Theory Comput.* **2009**, *5*, 993.
[39] L. Goerigk, S. Grimme, *J. Chem. Theory Comput.* **2010**, *6*, 107.
[40] T. Schwabe, R. Huenerbein, S Grimme, *Synlett* **2010**, *10*, 1431.
[41] H. L. Woodcock, H. F. Schaefer III, P. R. Schreiner, *J. Phys. Chem. A* **2002**, *106*, 11923.
[42] E. Johnson, O. J. Clarkin, G. A. DiLabio, *J. Phys. Chem. A* **2003**, *107*, 9953.
[43] A. J. Cohen, P. Mori-Sánchez, W. Yang, *Science* **2008**, *321*, 792.
[44] E. Johnson, P. Mori-Sánchez, A. J. Cohen, W. Yang, *J. Chem. Phys.* **2008**, *129*, 204112.
[45] T. Yanai, D. P. Tew, N. C. Handy, *Chem. Phys. Lett.* **2004**, *393*, 51.
[46] M. J. G. Peach, T. Helgaker, P. Sałek, T. W. Keal, O. B. Lutnæs, D. J. Tozer, N. C. Handy, *Phys. Chem. Chem. Phys.* **2006**, *8*, 558.
[47] M. J. G. Peach, E. I. Tellgren, P. Sałek, T. Helgaker, D. J. Tozer, *J. Phys. Chem. A* **2007**, *111*, 11930.
[48] P. A. Limacher, K. V. Mikkelsen, H. P. Lüthi, *J. Chem. Phys.* **2009**, *130*, 194114.
[49] S. Borini, P. A. Limacher, H. P. Lüthi, *J. Chem. Phys.* **2009**, *131*, 124105.
[50] M. F. Iozzi, T. Helgaker, E. Uggerud, *Mol. Phys.* **2009**, *107*, 2537.
[51] F. De Vleeschouwer, V. Van Speybroeck, M. Waroquier, P. Geerlings, F. De Proft, *Org. Lett.* **2007**, *9*, 2721.
[52] F. De Vleeschouwer, V. Van Speybroeck, M. Waroquier, P. Geerlings, F. De Proft, *J. Org. Chem.* **2008**, *73*, 9109.
[53] C. J. Parkinson, P. M. Mayer, L. Radom, *Theor. Chem. Acc.* **1999**, *102*, 92.
[54] D. J. Henry, C. J. Parkinson, P. M. Mayer, L. Radom, *J. Phys. Chem. A* **2001**, *105*, 6750.
[55] G. P. F. Wood, D. Moran, R. Jacob, L. Radom, *J. Phys. Chem. A* **2005**, *109*, 6318.
[56] E. I. Finkelshtein, *J. Phys. Org. Chem.* **2001**, *14*, 543.
[57] D. D. M. Wayner, K. B. Clark, A. Rauk, D. Yu, D. A. Armstrong, *J. Am. Chem. Soc.* **1997**, *119*, 8925.
[58] *Gaussian 03, Revision C.02*, M. J. Frisch, G. W. Trucks, H. B. Schlegel, G. E. Scuseria, M. A. Robb, J. R. Cheeseman, J. A. Montgomery, Jr., T. Vreven, K. N. Kudin, J. C. Burant, J. M. Millam, S. S. Iyengar, J. Tomasi, V. Barone, B. Mennucci, M. Cossi, G. Scalmani, N. Rega, G. A. Petersson, H. Nakatsuji, M. Hada, M. Ehara, K. Toyota, R. Fukuda, J. Hasegawa, M. Ishida, T. Nakajima, Y. Honda, O. Kitao, H. Nakai, M. Klene, X. Li, J. E. Knox, H. P. Hratchian, J. B. Cross, V. Bakken, C. Adamo, J. Jaramillo, R. Gomperts, R. E. Stratmann, O. Yazyev, A. J. Austin, R. Cammi, C. Pomelli, J. W. Ochterski, P. Y. Ayala, K. Morokuma, G. A. Voth, P. Salvador, J. J. Dannenberg, V. G. Zakrzewski, S. Dapprich, A. D. Daniels, M. C. Strain, O. Farkas, D. K. Malick, A. D. Rabuck, K. Raghavachari, J. B. Foresman, J. V. Ortiz, Q. Cui, A. G. Baboul, S. Clifford, J. Cioslowski, B. B. Stefanov, G. Liu, A. Liashenko, P. Piskorz, I. Komaromi, R. L. Martin, D. J. Fox, T. Keith, M. A. Al-Laham, C. Y. Peng, A. Nanayakkara, M. Challacombe, P. M. W. Gill, B. Johnson, W. Chen, M. W. Wong, C. Gonzalez, J. A. Pople, Gaussian, Inc., Wallingford CT, **2004**..
[59] Orca (Version 2.6), *An Ab Initio, DFT and Semiempirical Electronic Structure Package*, F. Neese, University of Bonn, Germany, **2008**.
[60] E. F. C. Byrd, C. D. Sherrill, M. Head-Gordon, *J. Phys. Chem. A* **2001**, *105*, 9736.
[61] M. L. Coote, *J. Phys. Chem. A* **2004**, *108*, 3865.
[62] *Gaussian 09, Revision A.02*, M. J. Frisch, G. W. Trucks, H. B. Schlegel, G. E. Scuseria, M. A. Robb, J. R. Cheeseman, G. Scalmani, V. Barone, B. Mennucci, G. A. Petersson, H. Nakatsuji, M. Caricato, X. Li, H. P. Hratchian, A. F. Izmaylov, J. Bloino, G. Zheng, J. L. Sonnenberg, M. Hada, M. Ehara, K. Toyota, R. Fukuda, J. Hasegawa, M. Ishida, T. Nakajima, Y. Honda, O. Kitao, H. Nakai, T. Vreven, J. A. Montgomery, Jr., J. E. Peralta, F. Ogliaro, M. Bearpark, J. J. Heyd, E. Brothers, K. N. Kudin, V. N. Staroverov, R. Kobayashi, J. Normand, K. Raghavachari, A. Rendell, J. C. Burant, S. S. Iyengar, J. Tomasi, M. Cossi, N. Rega, J. M. Millam, M. Klene, J. E. Knox, J. B. Cross, V. Bakken, C. Adamo, J. Jaramillo, R. Gomperts, R. E. Stratmann, O. Yazyev, A. J. Austin, R. Cammi, C. Pomelli, J. W. Ochterski, R. L. Martin, K. Morokuma, V. G. Zakrzewski, G. A. Voth, P. Salvador, J. J. Dannenberg, S. Dapprich, A. D. Daniels, Ö. Farkas, J. B. Foresman, J. V. Ortiz, J. Cioslowski, D. J. Fox, Gaussian, Inc., Wallingford CT, **2009**.
[63] Y. Tawada, T. Tsuneda, S. Yanagisawa, T. Yanai, K. Hirao, *J. Chem. Phys.* **2004**, *120*, 8425.
[64] O. A. Vydrov, G. E. Scuseria, *J. Chem. Phys.* **2006**, *125*, 234109.

[65] O. A. Vydrov, J. Heyd, A. Krukau, G. E. Scuseria, *J. Chem. Phys.* **2006**, *125*, 074106.
[66] O. A. Vydrov, G. E. Scuseria, J. P. Perdew, *J. Chem. Phys.* **2007**, *126*, 154109.
[67] R. G. Parr, L. Von Szentpaly, S. B. Liu, *J. Am. Chem. Soc.* **1999**, *121*, 1922.
[68] F. De Vleeschouwer, P. Jaque, P. Geerlings, A. Toro-Labbé, F. De Proft, *J. Org. Chem.* **2010**, *75*, 4964.
[69] F. De Vleeschouwer, F. De Proft, P. Geerlings, Invited contribution to *J. Mol. Struct. (THEOCHEM)*, Special issue on Conceptual DFT (Eds.: P. K. Chattaraj, A. J. Thakkar), **2010**, *943*, 94.
[70] a) A. E. Reed, R. B. Weinstock, F. Weinhold, *J. Chem. Phys.* **1985**, *83*, 735; b) A. E. Reed, F. Weinhold, *J. Chem. Phys.* **1985**, *83*, 1736; c) A. E. Reed, L. A. Curtiss, F. Weinhold, *Chem. Rev.* **1988**, *88*, 899.
[71] Neese and coworkers reported a slight increase of 4 kJ mol^{-1} from **5–13** to **5–14**, which is not in correspondence with our original computations where a much larger increase was observed for all investigated methods. More specifically, an increase of 18.6 kJ mol^{-1} was reported using the B2PLYP functional for the energy computations.[23] This discrepancy can be attributed to differences in the geometry optimization, as in ref. [28] the wrong electronic state was obtained for radical **5–13** (private communication with the authors of ref. [28]). The real ground state is found to be 9.8 kJ mol^{-1} lower in energy at the B3LYP-D/tzvp level of theory. This geometry corresponds with the one used in ref. [23]. Use of the correct geometry results in a bond dissociation energy value of 365.1 kJ mol^{-1} using B2PLYP-D/tzvpp//B3LYP-D/tzvp, which is 14.8 kJ mol^{-1} lower compared to the value reported in [28] (see behavior of the green circles in Figure 6).

Received: September 24, 2010
Revised: January 21, 2011
Published online on March 24, 2011

